2014 American Control Conference (ACC)
June 4-6, 2014. Portland, Oregon, USA

A Hybrid Controller for Autonomous Vehicle Lane Changing with Epsilon Dragging

Sean Whitsitt[1] and Jonathan Sprinkle[2]

Abstract— **Trajectory control for an autonomous ground vehicle typically utilizes the error from the desired path or trajectory (i.e., crosstrack error) to produce velocity and steering commands. If an obstacle is in the path, previous techniques have synthesized a new trajectory that avoids the obstacles, and the vehicle directly follows this new path. This approach has drawbacks at high velocity, because the synthesized trajectory must satisfy the stability criteria of the vehicle. This paper introduces a technique which we call epsilon dragging. The approach modifies the existing trajectory by some value ε in order to avoid an obstacle at high speeds, while preserving the original trajectory as the desired path. Epsilon dragging is performed by inducing an additional error to the crosstrack error of the vehicle; this induced error can be bounded in order to stay within the velocity/turnrate profile that governs safe behavior at high speeds. The paper provides a method to construct epsilon such that a vehicle can avoid an obstacle at high speeds without the need to verify the trajectory's curvature before it is synthesized. The technique is demonstrated in completing a lane-change maneuver at different velocities, and verifying that the velocity/turnrate profiles are not exceeded.**

I. Introduction

Crosstrack error is used in steering controllers to pull a vehicle towards a desired trajectory, and convergence of steering controllers for (small) crosstrack error has been established in the literature [4]. However, if the desired trajectory is disturbed for some reason (e.g. GPS error, or an offset to permit lane changing) the crosstrack error for the vehicle will receive a step input, which could cause the vehicle to perform unsafe or uncomfortable maneuvers.

Previous results depend on small crosstrack error, or a predefined maximum turn rate (at a fixed velocity), in the proof for stability of the steering controller. In previous work we have shown how to define a constraint for safe maneuvers which is a function of velocity and steering angle [10], but this constraint is not trivially shown to be met at variable speed if the trajectory is modified, for reasons we describe below.

This paper considers example maneuvers where a trajectory modification is required, such as changing lanes or avoiding an obstacle. We will refer to this maneuver throughout as a *lane change maneuver*, as avoiding a stationary obstacle directly in the path can be performed with the same maneuver, but with a lane width specified by the minimum deviation required to avoid the obstacle.

[1]Sean Whitsitt is with the Department of Electrical and Computer Engineering, University of Arizona, Tucson, AZ 85721, USA whitsitt@email.arizona.edu

[2]Jonathan Sprinkle is with the Department of Electrical and Computer Engineering, University of Arizona, Tucson, AZ 85721, USA sprinkle@ece.arizona.edu

A traditional approach to solving this problem is to modify the trajectory to be followed, and then follow the trajectory. This approach requires (1) that the updated trajectory be feasible, based on the vehicle's kinematic (or dynamic) model; (2) that the trajectory not result in the vehicle leaving its predefined safety region.

A more significant limitation is that, fundamentally, there are an infinite number of trajectories that avoid the obstacle, thus satisfying the overall goal. However, each of these may have different costs, if a predictive controller is used. That is, the cost of the deviation from the original path, plus any error in following that new path, may complicate systems that utilize optimizing controllers.

This motivates us to directly induce error into the steering controller, rather than modify the trajectory. This has the advantage of not requiring the vehicle model be used to generate a feasible trajectory: rather, the followed trajectory will be feasible, since the steering controller's inputs will be guaranteed to be within the safe region of the controller. Also, the error from the trajectory will appear only on a short horizon, so an MPC controller will not be adversely affected by a trajectory offset that might result in an optimized result that is in a local minimum.

II. Problem Description

We use two key previous results in this paper: a controller that generates steering angles for a given crosstrack error (at a certain velocity) [4], and a controller that constrains velocity to achieve a certain steering angle [10].

Consider the steering controller [8], [4],

$$\delta(t) = g(e, v, \psi) = \psi(t) + \arctan\frac{ke(t)}{v(t)} \tag{1}$$

where δ is the output steering angle, e is the distance to the closest point of the reference trajectory (or lateral distance to the path), ψ is the heading error to the tangent of the closest point of the reference trajectory, k is a gain parameter that is always a positive real number, and v is the vehicle velocity. A new $e^* \gg e$ produces a new output δ^* that decreases (as velocity increases), but which may still exceed the safe allowable tire angle at those speeds. These tire angle constraints are calculated in previous work [10]:

$$g(\delta, v) = \begin{bmatrix} \frac{K_{va}}{M_a} & -(K_{va}+K_{vd}) \end{bmatrix} \begin{bmatrix} \delta_a \\ v_a \end{bmatrix} + \begin{bmatrix} \frac{K_{vd}}{M_d} \end{bmatrix} \delta_d \tag{2}$$

where δ_a is the steering angle, δ_d is a new desired tire angle, v_a is the vehicle velocity, g is an acceleration gain, and the

978-1-4799-3274-0/$31.00 ©2014 AACC

other values are calculated based on runtime linearization of the curve in Fig. 1 at an operating point (δ_a, v_a). The M values are based on the linearized slope and the K values are arbitrary gains, see [10] for more details. The curve is derived from driving data; thus these data can only be used if relevant to the vehicle in which they was captured. In this way, a so-called "comfort controller" can be configurable by driver, or by road conditions, and different vehicles will have different data-driven profiles [10]. Essentially this curve shows the velocities and tire angles at which a driver feels comfortable turning.

Problem Statement

Demonstrate the stability of a hybrid controller that generates an e_ε value such that the steering controller

$$\delta(t) = g(e, v, \psi) = \psi(t) + \arctan \frac{k(e(t) + e_\varepsilon(t))}{v(t)} \quad (3)$$

safely transitions the vehicle to a new trajectory. To do this, we must: (i) determine when to "switch" to a new lane, (ii) calculate a time-varying value for e_ε, and (iii) demonstrate that $e_\varepsilon(t)$ will avoid the obstacle without sacrificing stability or path convergence, and (iv) demonstrate that the system remains within its region of safety.

The remainder of the paper presents a hybrid controller with these properties. We demonstrate that (without changing the vehicle's velocity) we can decide what error to inject into the steering controller in order to obey the constraints of the region of safety. We additionally show the stability properties of this controller, even as the error from the desired trajectory increases (this relaxes an assumption in previous work that this error would be sufficiently small). These stability properties are constructed with injected error values derived from the region of safety constraints, so they are known to preserve safe execution according to these constraints.

Assumptions: The velocity controller (2) alters the v based on the δ_a and δ_d such that the vehicle maintains a safe and comfortable speed at any given time. Due to space limitation, we assume a nominal trajectory with no curvature, but this can be relaxed in a longer version of the paper. We also assume that lateral localization within a lane is possible (i.e., not necessarily global position), and that the longitudinal distance to the obstacle (e.g., the vehicle being passed) is known. The obstacle's velocity can also vary.

III. Background

A. Related Work

We decouple lane-specific behavior of a vehicle into lane keeping, and lane changing, behaviors.

Both [7] and [2] introduce controllers for lane keeping. These controllers assume that the vehicle should attempt to stay in its current lane. These are the kinds of controller that can be used in a hybrid lane changing controller both before and after the transition between lanes.

A controller for a lane changing maneuver with a concentration on obstacle avoidance and detection is introduced in [5]. However, that work does not address the issue of velocity versus the tire angle while changing lanes. Instead it assumes that the vehicle will not adjust its heading fast enough to cause problems.

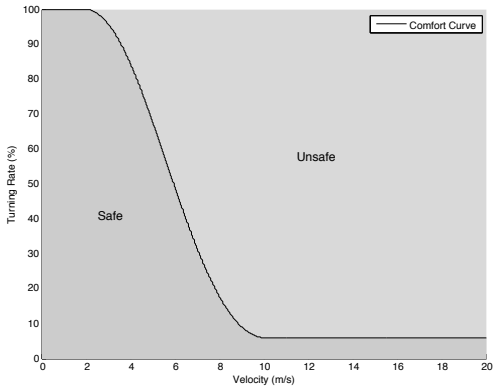

Fig. 1: Regions of safety across tire angle (δ) and vehicle velocity (v). Although the parameters of this curve vary by driver, it is of this archetypal shape.

In [1] a maneuver is proposed that uses a trapezoidal lateral acceleration profile to nudge the vehicle into the desired lane. The lateral acceleration of the vehicle is controlled such that the vehicle should not experience uncomfortable or unsafe lateral speeds. However, no attention is paid to proving that the motion is comfortable and safe, the values used are simply set low enough that they are believed to be safe.

A similar approach to that described herein can be found in [6]. This approach assumes that there is a lateral acceleration maximum that will put the vehicle into an unsafe and uncomfortable maneuver and the controller calculates the lane change trajectory based on this maximum. However, [6] admits lateral acceleration is a difficult state value to measure given the basic sensors available to a ground vehicle. Also, [6] does not take into account the other forces incident on the vehicle at the time which might cause issues with passenger comfort and safety.

Our approach differs since it uses velocity/tire angle data that are recorded under human control. Since these values were used safely before, they can be assumed to be safe given similar driving conditions. Different data for this safety region could be used in order to safely handle different driving conditions. Further, our constraints are directly on control inputs, whereas the work in [6] are on state variables that vary depending on the vehicle's equations of motion.

B. Vehicle Model

We use a simplified bicycle model to calculate the vehicle's state in our simulations [9]:

$$\begin{array}{lcllcl} \dot{x_1} & = & u_1 \cos(x_3)\cos(x_4) & \dot{x_2} & = & u_1 \cos(x_3)\sin(x_4) \\ \dot{x_3} & = & u_2 & \dot{x_4} & = & u_1 \frac{1}{L}\sin(x_3) \end{array} \quad (4)$$

where x_1 and x_2 are the x and y coordinates of the vehicle respectively, x_3 is the tire angle, x_4 is the heading, u_1 is the

vehicle velocity, u_2 is the angular rate of change of the tire angle, and L is the length of the vehicle. Note that the output of the steering controller in (1) is used to compute u_2. This is done based on the physical limitations for the angular rate of change for the vehicle's tire angle.

C. Region of Safety Calculations

Previous work [10] describes a controller for preventing a vehicle from performing unsafe turns by slowing the vehicle as it begins to perform the turn, and speeding up the vehicle as it exits the turn. This is referred to as the passenger comfort controller (PCC), which was briefly sketched in (2).

The PCC is derived from data recorded using a human driver. These data are then used to build a curve that defines the maximum allowable tire angle at any given velocity (Fig. 1). Note that at low velocities the data show that the vehicle's tire angle can take on any value. Larger than some velocity, the tire angle must remain small, but the velocity does not affect the maximum value of that tire angle. The results in [10] show this threshold value to be around 4% for the example vehicle and human driver used to collect data, though for other drivers this maximum value may vary.

The region of safety is derived from data, so different drivers, vehicles, driving conditions, etc., produce a different region of safety. The curve shown in Fig. 1 will exhibit different slopes or maxima in some regions if based on a different vehicle or driver, but all data sets collected have fit this archetypal function. The slope of the curve and the exact locations where it begins and ends its slope are the significant parameters that change between drivers of the same vehicle.

IV. Approach

This section discusses how the first three goals in the problem statement are achieved. The switching mechanism for goal (i) is discussed in Section IV-A. Epsilon dragging, which addresses goal (ii), is discussed in Section IV-B. The proof of stability for goal (iii) is discussed in Section IV-C.

A. The Hybrid System

Fig. 2 shows the two states for the hybrid controller and the transition conditions on those states. It is assumed that higher level conditions (e.g. an obstacle is in front with no obstacles to the side) have already been met.

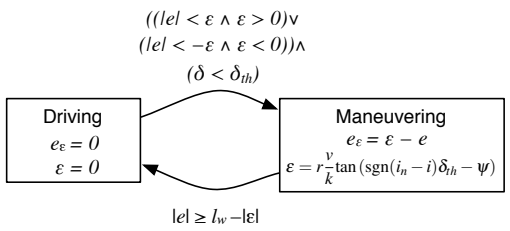

Fig. 2: The states for the hybrid system with transition conditions.

First, an additional vehicle state variable is necessary to identify the lane that the vehicle should be following. Let $i \in \mathbb{Z}$ be the current lane and $i_n \in \mathbb{Z}$ be the lane into which the vehicle is transitioning. For simplicity's sake there is one condition on the pair i and i_n given by $|i_n - i| \leq 1$, i.e., the vehicle will only transition by one lane.

1) The Driving State: The driving state is simply the state wherein the Hoffmann controller and PCC operate to control the vehicle and guide it along a given trajectory with no induced error (i.e. $e_\varepsilon = 0$).

2) Transitioning from Driving to Maneuvering: Assuming that the the vehicle has determined that it is both desirable to change lanes and there are no obstacles in the way, there are two conditions that must be met for the lane change to begin. First, the vehicle must be close to the center of the current lane (i.e. the vehicle's crosstrack error must be small). As such, consider the desired error value (ε) that will be used to drive the vehicle to the next lane. Assuming that this value has been constructed to allow the vehicle to safely transition and the magnitude of crosstrack error is smaller than this value, then the vehicle should be able to safely induce this error and begin the transition. Second, the concept of inducing this error value in the steering controller is based around preventing the vehicle from attaining a tire angle of greater magnitude than some threshold value (δ_{th}). Therefore, as long as the tire angle is below this threshold the vehicle can induce the error and begin the maneuver. Equation (5) shows this constraint mathematically.

$$((|e| < \varepsilon \wedge \varepsilon > 0) \vee (|e| < -\varepsilon \wedge \varepsilon < 0)) \wedge (\delta < \delta_{th}) \quad (5)$$

If the vehicle determines that it is desirable to change lanes and these conditions are satisfied then it can set $i_n = i \pm 1$ depending on the desired merging direction.

3) The Maneuvering State: This state is similar to the driving state in that the Hoffmann controller and PCC operate to control the vehicle, except now $e_\varepsilon \neq 0$.

4) Transitioning from Maneuvering to Driving: The maneuvering state only has to get the vehicle within ε of the next lane before the vehicle can safely latch onto the new path and use it over the old path. Using l_w as the width of a lane, (6) shows the condition by which the controller can set $i = i_n$ and return to the driving state in the new lane.

$$|e| \geq l_w - |\varepsilon| \quad (6)$$

B. Epsilon Drag

Definition 1: The lemma in Section IV-C shows that an error can be induced in the crosstrack error of an autonomous vehicle in order to force it to move laterally to its given desired path. Now, from (1) a desired value for this induced error can be derived based on the state of the vehicle. Remember from Section III-C that this value should keep the steering angle low enough to prevent the velocity controller from slowing the vehicle down.

First, (7) defines the threshold on the desired tire angle that will prevent the system from turning too much during this maneuver. The value for T_h is defined based on the velocity and the velocity controller of the vehicle. Note that the value for T_h is typically less than 0.05. Lastly, δ_{max} is the maximum

allowable tire angle for the vehicle based on physical or other constraints (i.e., the tires of a vehicle can only turn in a limited range).

$$|\delta_{th}| < T_h|\delta_{max}| \quad 0 \leq T_h \leq 1 \tag{7}$$

By plugging information from (7) into (1) and solving for (e) a maximum value (ε) for the crosstrack error can be defined as in (8). Note that $\text{sgn}(i_n - i)$ indicates the direction of the induced error (i.e. if the vehicle should merge to the left then $\text{sgn}(i_n - i) = 1$ whereas $\text{sgn}(i_n - i) = -1$ means merge right). In (8), r is a factor that limits the ε such that it does not actually reach the threshold value. This prevents the vehicle from turning quickly enough to interfere with the passenger comfort controller [10] for the vehicle. The value is mostly arbitrary, but a smaller r value will decrease the rate at which the vehicle maneuvers between lanes while a higher value will increase the rate.

$$\varepsilon = r\frac{v}{k}\tan\left(\text{sgn}(i_n - i)\delta_{th} - \psi\right) \quad 0 \leq r \leq 1 \tag{8}$$

The value ε is the value at which the vehicle should keep the crosstrack error that is injected into the Hoffmann controller in order to transition between lanes. The relationship between this desired error and the error that should be induced into the system in order to actually manage the transition is given by $e_\varepsilon = \varepsilon - e$.

C. The Steering Controller Global Asymptotic Stability

Theorem 1: The Hoffmann steering controller given by (1) is globally asymptotically stable for all crosstrack error.

Proof: Using the bicycle vehicle dynamics (4) and the steering controller (1) it can be shown that the vehicle has the dynamics given by (9) for its crosstrack error (see [3] for the proof of this). [4] also shows that the only equilibrium point of this system is the origin where crosstrack error and heading error are both 0. Fig. 3 shows the lane changing maneuver with the crosstrack error labeled as e.

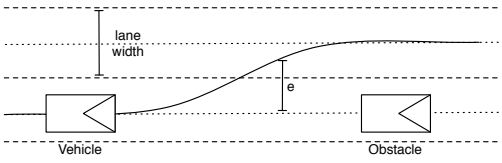

Fig. 3: The lane change maneuver where e is crosstrack error.

$$\dot{e} = -v\sin\left(\text{atan}\left(\frac{ke}{v}\right)\right) = \frac{-ke}{\sqrt{1+\left(\frac{ke}{v}\right)^2}} \tag{9}$$

For small e (9) can be estimated by $\dot{e} = -ke$, which has a simple exponential equation as a solution. Ideally, the crosstrack error will always stay bounded in a way such that this estimation is good enough to give stability for the whole system. However, this proof can be further expanded by finding a Lyapunov equation (V) that shows the equation is globally asymptotically stable (GAS) to the origin (where $e = 0$).

Note that $V(e) = |e|$ fits with the definition of a global Lyapunov equation (i.e. it is globally positive definite $|0| = 0$ and $|e| > 0\ \forall e \in \mathbb{R}\backslash\{0\}$). $\dot{V}(e) = \text{sgn}(e)\dot{e}$ can be derived using V and (9).

Now, it can be simply seen that (9) has a sign dependent only on e since its denominator is always positive and k is defined as a positive number (which is the opposite of the sign of $\dot{e}$). As such, $\dot{V}$ is globally negative semidefinite and as a result (9) is GAS.

■

Lemma 1: The Hoffmann steering controller with an error term added to the crosstrack error is globally asymptotically stable for all crosstrack error.

Proof: Above is the proof that (1) is stable for any given crosstrack error. From this it can be shown that if the crosstrack error is perturbed or otherwise adjusted then the function is still stable, but that the equilibrium point changes. Using $e^* = e + e_\varepsilon$ as the new coordinates, (10) shows the perturbed system.

$$\delta(t) = \psi(t) + \arctan\frac{k(e(t)+e_\varepsilon(t))}{v(t)} = \psi(t) + \arctan\frac{ke(t)^*}{v(t)} \tag{10}$$

Plugging these new coordinates in yields an equation of the same form as the original, i.e., it is GAS to the origin of e^* which is the point at which $e + e_\varepsilon = 0$.

■

V. Results

This section demonstrates that the system operates within the defined regions of safety and meets goal (iv) of the problem statement. Initial simulations based on the epsilon dragging lane changing controller show promising results for a vehicle operating at high speeds. However, the rest of this section will show that while in all cases this controller meets the goal of developing a hybrid controller that does not affect the velocity of the vehicle, the controller leaves some room for improvement at low speeds.

A. Simulation Setup

Each simulation described herein was set up in the same manner. At the start of the simulation, the vehicle is traveling down the center of a straight lane at the desired velocity. At 50 meters into the simulation the lane change maneuver is begun and the vehicle transitions to the left. The lane width (l_w) is defined as 3 meters. The maximum tire angle (δ_{max}) is defined as 24°. The simulation path is 1 kilometer long and the simulation is run for 200 seconds or the vehicle reaches the end of the path, whichever occurs first. A gain (k) value of 0.5 is used for the steering controller, and the PCC is primed with the data shown in Fig. 1. The rate (r) used for the induced error values is defined as 0.3. The values for k and r are mostly arbitrary. However, higher values for r will result in a faster convergence to the opposing lane (note that this paper does not explore the effects of alternate selections of these values). Also, the vehicle is arbitrarily set to transition to the left, in assuming that the vehicle has determined it is safe to transition it is also assumed that it has determined a safe direction to transition as well. Using these parameters, four different simulations were run varying the velocity between 4 m/s, 8 m/s, 30 m/s, and 60 m/s.

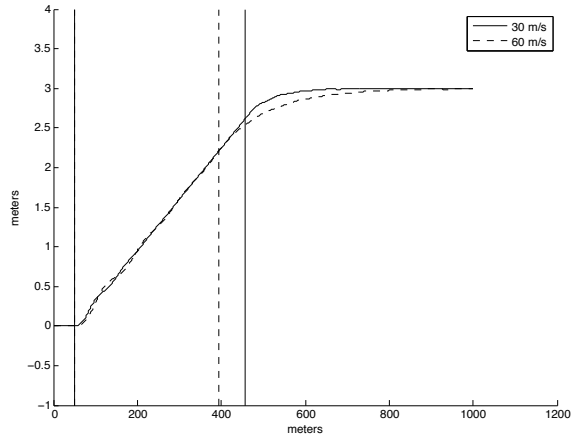

(a) The path of the vehicle while changing lanes at high speeds. The vehicles are traveling from the left of the graph to the right.

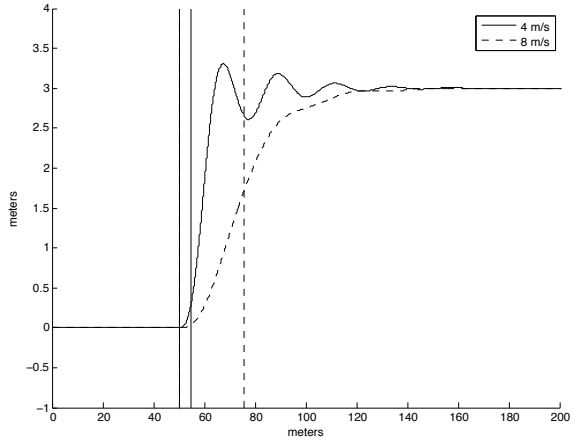

(b) The path of the vehicle while changing lanes at low speeds. The vehicles are traveling from the left of the graph to the right.

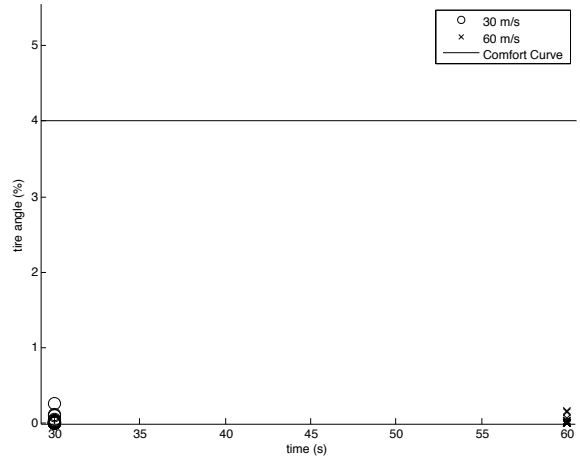

(c) The comfort curve and the tire angle as a percentage of the maximum tire angle versus the velocity during the high speed maneuvers.

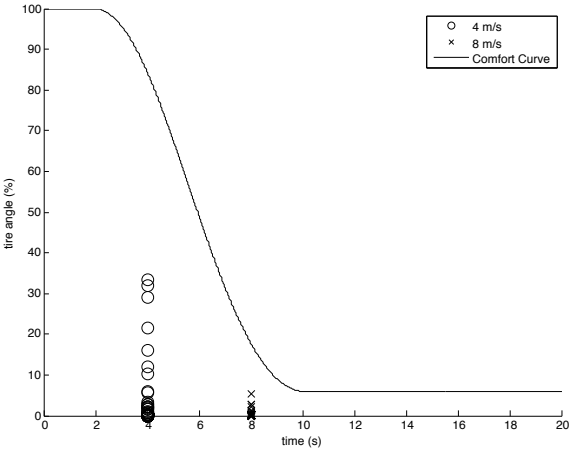

(d) The comfort curve and the tire angle as a percentage of the maximum tire angle versus the velocity during the low speed maneuvers.

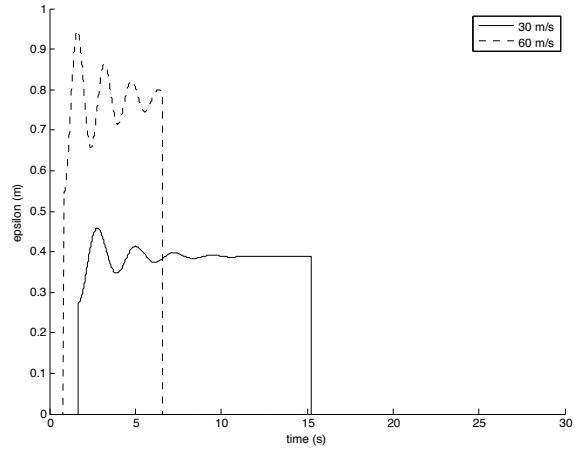

(e) The value of the desired crosstrack error for the high speed simulations during the maneuver.

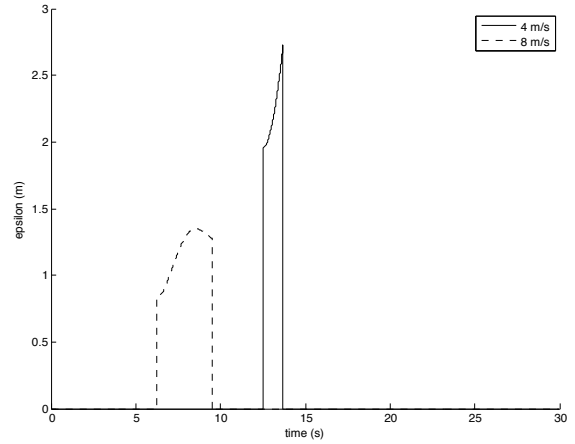

(f) The value of the desired crosstrack error for the low speed simulations during the maneuver.

Fig. 4: The results of the four simulations.

B. High Speed Simulations

Fig. 4a shows the path the vehicle takes to get from one lane to the next at both 30 m/s and 60 m/s. The two paths are nearly identical because of the assumption made from previous work as discussed in Section III-C that at high velocities there is a threshold tire angle that the vehicle can operate up to without necessitating modifications to its velocity. As such, this path will look similar to those in Fig. 4a for all velocities above which Fig. 1 reaches that tire angle threshold. With respect to these data that velocity value is about 9.8 m/s. The tire angle threshold is about 4% of the maximum tire angle, or about 0.96°. Using a different curve would result in both a different tire angle threshold and a different maximum velocity. The vertical lines on the figure indicate the points on the path that the vehicle transitioned between states. For both cases, the line on the left at 50 meters is where the simulation transitions from driving to maneuvering. The lines on the right indicate where the maneuver ends for both high speed vehicles.

Fig. 4c shows the relationship between the tire angle and the velocity during the high speed simulations plotted with the PCC curve. Note that the velocity for both simulations never changes while the tire angle is free to move around. As such, the velocity during this maneuver is independent from the steering of the vehicle as intended.

Fig. 4e shows the desired crosstrack error during the maneuver with the high simulation velocities. Vehicle velocity has an impact on these values (see (8)). As would be expected from the equation for ε, doubling the velocity of the vehicle independently of the other variables also doubled the average value for the desired error. However, the faster vehicle had a larger oscillation in values for ε. This is because the system reacts more aggressively to larger crosstrack error as can be seen in (9). Near the origin of this equation, higher magnitudes of crosstrack error lead to higher magnitude values from the arctangent function and thus to higher magnitudes of tire angle.

C. Low Speed Simulations

Fig. 4b shows the path the vehicle takes to get from one lane to the next at both 4 m/s and 8 m/s. In this instance the slower speed has a more difficult time adjusting to the lane change and thus oscillates more. This is because (8) generates larger values for epsilon at low velocities. This does not appear to be the case at first glance, but consider the value for δ_{th}. Based on the PCC, this value can be large at low velocities which in turn leads to large values for ε. At 4 m/s, δ_{th} is about 76°. The large value for ε then allows the system to latch onto the next lane much more quickly than desired as indicated by the vertical solid lines in Fig. 4b that indicate that the maneuver ended very soon after it began. This results in the oscillating path that eventually converges onto the new lane. The dashed lines in the figure indicate that this problem begins to disappear and converge on a path similar to the high speed paths as the velocity increases.

Fig. 4d shows the tire angle versus the velocity during the low speed simulations along with the PCC curve. Note that in these cases the tire angle threshold value is higher than in the high speed simulations, but still safe.

Fig. 4f shows the desired crosstrack error during the lane changing maneuver at the high simulation velocities. Comparing this figure to Fig. 4e confirms the statement above that lower velocities lead to high values of desired crosstrack error as based on (8).

VI. Conclusion

This paper presents a hybrid controller that permits a lane-change maneuver to be performed by injecting error into the nominal trajectory, rather than synthesizing a new trajectory to follow. The inputs to an autonomous vehicle that will steer according to this error function are shown to be within the boundary of the region of safety for high speed maneuvers, since the error function is derived from the data that define this boundary. Simulation results show that the four design goals have been accomplished, namely that the controller transitions occur independently of the desired vehicle velocity by maintaining the tire angle within the safe region of the PCC. In future work we will improve the controller such that the tire angle during the maneuver is smoother, and that to avoid oscillation at low speed.

Acknowledgements

The authors thank Ricardo Sanfelice, who generously provided useful insight and comments into the description of the problem statement and the relevance of the work. This work is supported by the National Science Foundation award CNS-1253334.

References

[1] W. Chee and M. Tomizuka. Lane change maneuver of automobiles for the intelligent vehicle and highway system (IVHS). In *American Control Conference, 1994*, volume 3, pages 3586–3587 vol.3, 1994.

[2] K.-T. Feng, H.-S. Tan, and M. Tomizuka. Automatic steering control of vehicle lateral motion with the effect of roll dynamics. In *American Control Conference, 1998. Proceedings of the 1998*, volume 4, pages 2248–2252 vol.4, 1998.

[3] T. Gillespie. *Fundamentals of Vehicle Dynamics*. SAE International, 1992.

[4] G. Hoffmann, C. Tomlin, M. Montemerlo, and S. Thrun. Autonomous automobile trajectory tracking for off-road driving: Controller design, experimental validation and racing. In *American Control Conference, 2007. ACC '07*, pages 2296–2301, 2007.

[5] J. Kaneko and A. Shimamura. A design of lane change maneuver for automated vehicles. In *Decision and Control, 1998. Proceedings of the 37th IEEE Conference on*, volume 1, pages 1031–1033 vol.1, 1998.

[6] J.-W. Lee and B. Litkouhi. A unified framework of the automated lane centering/changing control for motion smoothness adaptation. In *Intelligent Transportation Systems (ITSC), 2012 15th International IEEE Conference on*, pages 282–287, 2012.

[7] E. P. Ping and S. K. Swee. Simulation and experiment of automatic steering control for lane keeping manoeuvre. In *Intelligent and Advanced Systems (ICIAS), 2012 4th International Conference on*, volume 1, pages 105–110, 2012.

[8] S. Thrun et al. Winning the DARPA Grand Challenge. *Journal of Field Robotics*, 23(9):661692, September 2006.

[9] G. Walsh, W. Tilbury, S. Sastry, R. Murray, and J. P. Laumond. Stabilization of trajectories for systems with nonholonomic constraints. *IEEE Transactions on Automatic Control*, 39:216–222, 1994.

[10] S. Whitsitt and J. Sprinkle. A passenger comfort controller for an autonomous ground vehicle. In *51st IEEE Conference on Decision and Control*, pages 3380–3385, 2012.